Research Paper
Computational Methods for Differential Equations
http://cmde.tabrizu.ac.ir
Vol. *, No. *, *, pp. 1-19
DOI:10.22034/cmde.2026.68654.3337

The dynamics of delayed population systems with age-selective Harvesting: interactions between stability, bifurcations, and bio-economic efficiency

Atish Kumar Sethy and Jyotiska Datta*
Department of Mathematics, Central University of Odisha-763004, Koraput, Odisha, India.

Abstract

This study examines the dynamic behaviour of salmon populations using the Leslie-Gower model, incorporating a Beddington-DeAngelis type functional response and non-linear harvesting targeting prey beyond a certain age. The analysis addresses several key aspects, including optimal harvesting strategies, bionomics equilibrium, Maximum Sustainable Yield (MSY), and qualitative dynamics of the system. Special attention is given to the asymptotic stability and delay-dependent nature of the internal equilibrium. A Hopf bifurcation is identified in relation to the maturation delay. To determine an optimal harvesting trajectory after reaching the MSY, Pontryagin's maximum principle is applied, with the existence of the bionomic equilibrium also taken into account. Numerical simulations are employed to further elucidate the system's behaviour and gain deeper insights into its dynamics.

Keywords. Singular optimal control, MSY, Hopf-bifurcation, Age-selective harvesting with generalist predators.
2010 Mathematics Subject Classification. 37G15, 37M10, 34C23, 93C43.

1. Introduction

After spending their early life stages in rivers, *salmon* migrate to the sea, where they attain maturity and undergo substantial increases in body mass. Upon reaching adulthood, *northern pike* return to freshwater rivers to spawn. In their native habitats, comprising lakes, streams, and rivers, these fish are highly valued as game species. For millennia, northern pike have coexisted with other indigenous species in regions located north and west of the Alaska Range. As opportunistic generalist predators, pike exhibit a broad dietary spectrum that includes freshwater salmon [19].

The seasonal return of salmon to Alaskan streams is essential not only for maintaining ecological balance but also for supporting one of the state's most significant commercial industries and for sustaining traditional subsistence lifestyles in rural communities. To inform management decisions, state biologists collect comprehensive datasets on commercial salmon fisheries, emphasising the sustainable use of fish resources for both ecological and subsistence purposes.

A similar socio-ecological dynamic can be observed in the Sundarban Mangrove ecosystem and the *Hooghly River*, where Hilsa fish Tenualosa ilisha play a vital economic and cultural role. In these ecosystems, Hilsa and other coexisting species occupy distinct trophic levels and act as generalist predators. Skilled Hilsa fishermen contribute substantially to both domestic and commercial fisheries, ensuring a continuous link between local livelihoods and resource sustainability [9, 11].

Understanding fish behaviour, such as migration, foraging, and habitat preferences, is critical for optimising fishing strategies. Effective fisheries management requires aligning harvesting techniques with the biological and ecological traits of target species. Among these, age and body size are particularly influential, as they determine growth rates, reproductive success, and mortality patterns [1]. Over recent decades, fisheries management paradigms have alternated between caution and optimism. Central to contemporary management frameworks is the concept of age-selective harvesting, an approach designed to achieve the Maximum Sustainable Yield (MSY) through adjustments in fishing effort, gear selectivity, and stock assessment parameters [17].

Received: 14 August 2025; Accepted: 11 July 2026.
∗ Corresponding author. Email: jyotiska.datta@gmail.com.

MSY, together with socio-economic and ecological considerations, has become a cornerstone of sustainable fisheries management [2, 5, 8, 18, 21, 28]. Efficient harvesting, whether age or size selective, plays a vital role in reducing population oscillations by converting overcompensatory dynamics into stable compensatory dynamics.

Following this perspective, Jana et al. [11, 12, 14, 24, 29] developed an age-selective harvesting model building on the foundational work of Arino et al. [4, 25], who analysed the combined effects of harvesting and delay in prey-predator systems. Motivated by these studies, the present work extends this framework by formulating a delay-based predator-prey model inspired by the Leslie-Gower model. In our formulation, the prey population grows logistically and is subjected to harvesting once it reaches a specified age. The predator-prey interaction follows the Beddington-DeAngelis functional response, expressed as

$$f(N) = \frac{eNP}{aN + bP + c}, \tag{1.1}$$

where e, a, b, and c denote the catching rate, handling time, predator interference coefficient, and saturation level, respectively [1, 6, 15, 20, 22, 23].

We incorporate two harvesting strategies frequently discussed in the literature:

(i) **Nonlinear harvesting:** $h(N) = \dfrac{qEN}{m_1E + m_2N}$, and

(ii) **Proportionate harvesting:** $h(N) = qEN$,

where q represents the catch-ability coefficient, E is the harvesting effort (e.g., number of boats or nets), and $m_1, m_2 > 0$ are constants relating to the effort harvest ratio at high stock levels [30]. Section 2 presents the formulation of the proposed model. The stability properties of the delayed system are analysed in Section 3. Section 4 is devoted to the study of optimal control and the bio-economic equilibrium under sustainability constraints, with particular emphasis on policies designed to achieve the maximum sustainable yield (MSY) and long-term economic viability. Numerical simulations are provided in section 5 to support the analytical results, and concluding remarks are given in section 6.

2. The proposed model

Here we describe the Leslie-Gower predator-prey model with a Beddington-DeAngelis type functional response as

$$\frac{dN}{dT} = rN\left(1 - \frac{N}{K}\right) - \frac{eNP}{aN + bP + c}, \tag{2.1a}$$

$$\frac{dP}{dT} = sP\left(1 - \frac{nP}{N}\right), \tag{2.1b}$$

where $N(0) > 0$ and $P(0) > 0$ are the initial conditions. Here, $N \equiv N(T)$ and $P \equiv P(T)$ represent the population densities of prey and predator at time T, respectively. The feasible region of the system (2.1) is defined as

$$\mathbb{R}_+{}^2 = \{(N, P) \in \mathbb{R}^2 \mid N \geq 0, P \geq 0\}. \tag{2.2}$$

All model parameters are assumed to be non-negative, and their biological interpretations are summarised in Table 1.

The Beddington-DeAngelis functional response, given by $f(N) = \dfrac{eNP}{aN + bP + c}$, characterises the predator–prey interaction. The prey population influences the predator's survival capacity, and thus the predator's carrying capacity K_P is considered proportional to prey abundance, i.e., $K_P = \dfrac{N}{n}$. Incorporating non-linear harvesting $H(N) = \dfrac{qEN}{m_1E + m_2N}$ into system (2.1), the modified model [30] takes the form

$$\frac{dN}{dT} = rN\left(1 - \frac{N}{K}\right) - \frac{eNP}{aN + bP + c} - \frac{qEN}{m_1E + m_2N}, \tag{2.3a}$$

$$\frac{dP}{dT} = sP\left(1 - \frac{nP}{N}\right), \tag{2.3b}$$

subject to the initial conditions $N(0) = N_0 > 0$, $P(0) = P_0 > 0$. Each individual's catchability coefficient and the corresponding harvesting effort are denoted by q and E, respectively, while m_1 and m_2 are positive constants. The

TABLE 1. Biological meaning of non-negative parameters.

Parameter	Biological interpretation
r	Intrinsic growth rate of the prey species, representing the difference between natural birth and mortality rates.
s	Intrinsic growth rate of the predator species.
K	Environmental carrying capacity for the prey population.
n	Number of prey required to maintain one predator at equilibrium.
a	Average time spent by predators in handling each prey.
b	Measure of mutual interference among predators.
c	Saturation constant for the functional response.
e	Capture rate or searching efficiency of the predator.
m_1, m_2	Non-negative constants related to the effort to harvest ratio at high stock levels.
q	Catch-ability coefficient, describing the efficiency of fishing effort.
E	Harvesting effort (e.g., number of boats or nets used).

system is well-defined in the positive quadrant $\mathbb{R}^2_+$ for $(\frac{m_1}{m_2})E < N$. For the non-delayed version, Zhang et al. [30] analysed the local and global stability properties. To account for the maturation delay in the prey population, the harvesting term is modified following [3, 10, 11], leading to the delay differential model

$$\frac{dN}{dT} = rN\left(1-\frac{N}{K}\right) - \frac{eNP}{aN+bP+c} - \frac{qEN(T-\tau)}{m_1\mu Ee^{\mu\tau} + \{m_1\rho E(e^{\mu\tau}-1)+m_2\mu\}N(T-\tau)}, \tag{2.4a}$$

$$\frac{dP}{dT} = sP\left(1-\frac{nP}{N}\right). \tag{2.4b}$$

The logistic growth law of prey is expressed as

$$\frac{dN}{dT} = rN\left(1-\frac{N}{K}\right) = rN - r\frac{N^2}{K} = \xi N - \mu N - \rho N^2,$$

where $r = \xi - \mu$ and $\rho = \frac{r}{K}$. Introducing the non-dimensional variables

$$N = kx, \quad P = \frac{rKY}{m}, \quad t = rT,$$

and defining the parameters

$$h = \frac{qE\mu}{rK\{m_1\rho E(e^{\mu\tau}-1)+m_2\mu\}}, \quad c = \frac{m_1\mu Ee^{\mu\tau}}{K\{m_1\rho E(e^{\mu\tau}-1)+m_2\mu\}},$$

$$\alpha = \frac{eK}{M}, \quad \sigma = aK, \quad \gamma = \frac{bKr}{m}.$$

We obtain the dimensionless system

$$\frac{dx}{dt} = x(1-x) - \frac{\alpha xy}{\sigma x+\gamma y+c} - \frac{hx(t-\tau)}{c_1+x(t-\tau)}, \tag{2.5a}$$

$$\frac{dy}{dt} = \delta y\left(1-\frac{\beta y}{x}\right). \tag{2.5b}$$

The delay system (2.5) with the subject to the initial conditions;

$$x(t) = \phi_1(t) \geq 0, \quad y(t) = \phi_2(t) \geq 0, \quad t \in [-\tau, 0], \quad \phi_1(0) > 0, \ \phi_2(0) > 0, \tag{2.6}$$

and all parameters are non-negative.

3. Analysis of the model system

3.1. **Positivity and boundedness of solutions.** With the initial conditions (2.6), integrating Eq. (2.5) we the following:

$$x(t) = x(0)\exp\left\{\int_0^t\left[x(s)(1-x(s)) - \frac{\alpha x(s)y(s)}{\sigma x(s)+\gamma y(s)+c} - \frac{hx(s-\tau)}{c_1+x(s-\tau)}\right]ds\right\} > 0,$$
$$y(t) = y(0)\exp\left\{\int_0^t \delta\left(1-\frac{\beta y(s)}{x(s)}\right)ds\right\} > 0.$$

Hence, whenever the system satisfies the initial conditions (2.6), we have $x(t) > 0$ and $y(t) > 0$ for all $t \geq 0$. Consequently, the interior of the first quadrant forms an invariant set for the delayed system described in Equation (2.5).

$$\frac{dx}{dt} \leq x(1-x),$$

which gives

$$\lim_{t\to\infty} \sup x(t) \leq 1.$$

Now, define a continuous function $\eta(t) = x(t) + y(t-\tau)$. Subsequently,

$$\frac{d\eta(t)}{dt} + \mu\eta(t) = x(\mu+1-x) - \frac{\alpha xy}{\sigma x+\gamma y+c} - \frac{hx(t-\tau)}{c_1+x(t-\tau)} + (\delta+\mu)y(t-\tau) - \delta\beta\frac{y^2(t-\tau)}{x(t-\tau)}.$$

Therefore,

$$\frac{d\eta(t)}{dt} + \mu\eta(t) \geq \frac{(\mu+1)^2}{4} + \frac{(\delta+\mu)^2}{4\delta\beta} = \sigma_1.$$

Hence,

$$0 < \eta(t) < \frac{\sigma_1}{\mu}(1-e^{-\mu t}) + \eta(0)e^{-\mu t}, \tag{3.1}$$

and for $t \to \infty$, $0 < \eta(t) < \frac{\sigma_1}{\mu}$. Therefore, $\eta(t)$ is bounded. Consequently, from the definition of $\eta(t)$, any solution of system (2.5) is bounded.

3.2. **Stability of the delayed system.** The system (2.5) possesses a single interior equilibrium point denoted by $E_*(x_*, y_*)$, where $y_* = \dfrac{x_*}{\beta}$ and x_* is the positive root of the equation

$$Ax^3 + Bx^2 + Cx + D = 0, \tag{3.2}$$

where

$$A = \alpha + \frac{\gamma}{\beta}, \quad B = c_1\sigma + \frac{c_1\gamma}{\beta} - \frac{\gamma}{\beta} - \alpha + c, \quad C = \frac{\alpha}{\beta} - \frac{c_1\gamma}{\beta} - c_1\sigma + c_1c - c, \quad D = c_1c - h.$$

Since both c_1 and h depend on the delay parameter (τ), the equilibrium point also depends on (τ).

Linearize system (2.5) at $E_*(x_*, y_*)$, we obtain the following:

$$\frac{dx}{dt} = a_{11}x(t) + a_{12}y(t) + b_{11}x(t-\tau),$$
$$\frac{dy}{dt} = a_{21}x(t) + a_{22}y(t), \tag{3.3}$$

where

$$a_{11} = 1 - 2x_* - \frac{\alpha\gamma y_*^2 + c\alpha y_*}{(\sigma x_* + \gamma y_* + c)^2}, \quad a_{12} = -\frac{\alpha\sigma x_*^2 + c\alpha x_*}{(\sigma x_* + \gamma y_* + c)^2},$$
$$a_{21} = \frac{\delta\beta y_*^2}{x_*^2}, \quad a_{22} = \delta - \frac{2\delta\beta y_*}{x_*}, \quad b_{11} = -\frac{c_1 h}{(c_1 + x_*)^2}.$$

The corresponding characteristic equation is given by

$$\lambda^2 + P\lambda + Q + e^{-\lambda\tau}(R\lambda + S) = 0, \tag{3.4}$$

where

$$P = -(a_{11} + a_{22}), \quad Q = a_{11}a_{22} - a_{12}a_{21}, \quad R = -b_{11}, \quad S = b_{11}a_{22}.$$

If ω satisfies the condition that $i\omega$ ($\omega > 0$) is a root of Eq. (3.4), then

$$(-\omega^2 + Q + R\omega\sin\omega\tau + S\cos\omega\tau) + i(P\omega + R\omega\cos\omega\tau - S\sin\omega\tau) = 0. \tag{3.5}$$

Separating the real and imaginary parts, we obtain

$$\begin{aligned} \omega^2 - Q &= R\omega\sin\omega\tau + S\cos\omega\tau, \\ -P\omega &= R\omega\cos\omega\tau - S\sin\omega\tau. \end{aligned} \tag{3.6}$$

The roots of Eq. (3.4) are purely imaginary for positive τ and ω. Squaring and adding these equations, we get the following

$$\omega^4 + p\omega^2 + q = 0, \tag{3.7}$$

where $p = P^2 - 2Q - R^2$ and $q = Q^2 - S^2$.

We now determine the critical delay value τ_k at which the system (2.5) changes stability. From Eq. (3.6), we obtain

$$\tau_k = \frac{1}{\omega_k}\cos^{-1}\left[\frac{(S - PR)\omega_k^2 - SQ}{S^2 + R^2\omega_k^2}\right] + \frac{2k\pi}{\omega_k}, \tag{3.8}$$

where $k = 0, 1, 2, \ldots$ and ω_k denotes the unique positive root of Eq. (3.7). Define $\theta(\tau) \in [0, 2\pi]$ so that the right-hand side of the defining relation yields $\cos\theta(\tau)$. The values of τ corresponding to stability switches are the solutions of

$$S_k(\tau) = \tau - \tau_k. \tag{3.9}$$

Furthermore, differentiating Eq. (3.4) with respect to τ, we get

$$\left[\Re\left(\frac{d\lambda}{d\tau}\right)^{-1}\right]_{\omega=\omega_0,\tau=\tau_0} = \frac{2\omega_0^4 + p\omega_0^2}{R^2\omega_0^4 + S^2\omega_0^2} > 0, \tag{3.10}$$

since $p > 0$.

Theorem 3.1. *Assume $\tau > 0$ and that the conditions for the asymptotic stability of the non-delayed counterpart of system (2.5) ($\tau = 0$) are satisfied [7, 30]. Then the equilibrium point $E_*(x_*, y_*)$ of the system (2.5) is locally asymptotically stable for $\tau < \tau_0$ and unstable for $\tau > \tau_0$. Furthermore, at $\tau = \tau_0$, the system (2.5) undergoes a Hopf bifurcation at $E_*(x_*, y_*)$, where*

$$\tau_0 = \frac{1}{\omega_0}\cos^{-1}\left[\frac{(S - PR)\omega_0^2 - SQ}{S^2 + R^2\omega_0^2}\right].$$

4. Sustainable policy and MSY policy

Maximum sustainable yield (MSY) refers to the highest annual catch that a prey species can support over time while maintaining a stock level that optimises growth. This yield fluctuates over time depending on the ecosystem's requirements for self-sustenance. Several factors impose constraints on this yield.

In this context, the total yield ($Y(E^T)$) at the equilibrium point $E_*(x_*, y_*)$ is given by

$$Y(E^T) = Ex_*. \tag{4.1}$$

The properties of the total yield ($Y(E^T)$) are influenced by both τ and x_*, which are functions of E, and their explicit expressions are highly complex.

4.1. **Bionomic equilibrium.** Economic forces such as supply and demand for goods and services play a crucial role in determining economic equilibrium. When these forces are balanced, economic equilibrium is achieved. In this state, external influences do not affect the system until a key economic variable changes.

The method of age-selective harvesting, a central concept in fisheries management, significantly influences both biological and economic equilibrium. In the context of the biogenetic equilibrium of the model system (2.5), the cost per unit of effort, denoted by c_2, and the price per unit biomass of prey, denoted by p_1, are key parameters influencing the dynamics of prey.

At any given time, net revenue R—often referred to as net economic rent—can be expressed as

$$R = (\frac{p_1 h_1 x}{c_1 + x} - c_2)E,$$

where $h_1 = \dfrac{q\mu}{rK\{m_1\rho E(e^{\mu\tau} - 1) + m_2\mu\}}$.

The simultaneous equations that define the bionomics equilibrium $(x_\infty, y_\infty, E_\infty)$ are given by

$$\begin{aligned} x(1-x) - \frac{\alpha xy}{\sigma x + \gamma y + c} - \frac{hx}{c_1 + x} &= 0, \\ \delta y(1 - \frac{\beta y}{x}) &= 0, \\ (\frac{p_1 h_1 x}{c_1 + x} - c_2)E &= 0. \end{aligned} \tag{4.2}$$

To identify the bionomics equilibrium, we examine the following scenarios,

Case 4.1. When the cost of the prey exceeds its revenue ($c_2 > \frac{p_1 h_1 x}{c_1 + x}$), it becomes impractical to harvest the prey, and harvesting is halted ($E = 0$).

Case 4.2. If $c_2 < \frac{p_1 h_1 x}{c_1 + x}$, the prey yields positive revenue, implying that the system is biologically and economically feasible. The ideal harvesting levels are

$$x_\infty = \frac{c_1 c_2}{p_1 h_1 - c_2}, \quad y_\infty = \frac{c_1 c_2}{\beta(p_1 h_1 - c_2)}, \quad E_\infty = \frac{\Omega K m_2 x_\infty}{qrK - \{m_1\mu e^{\mu\tau} + m_1\rho K(e^{\mu\tau} - 1)x_\infty\}\Omega K},$$

where $\Omega = 1 - x_\infty - \dfrac{\alpha y_\infty}{\sigma x_\infty + \gamma y_\infty + c}$.

4.2. **Optimal harvesting policy.** Optimal harvesting strategies have gained significant attention in bio-mathematics due to their importance in integrating economic considerations into population models and resource management. The main goal is to maximise profit while minimising effort. Clark made foundational contributions to this area, and later explored optimal harvesting in a stochastic framework. In this section, we apply an instantaneous yearly discount rate, denoted by ξ, to define the objective functional of the harvesting model to be maximised as

$$J(E) = \int_0^\infty e^{-\xi t} \left(\frac{p_1 h_1 x}{c_1 + x} - c_2 \right) E \, dt, \tag{4.3}$$

subject to control constraints (2.5) and state constraints

$$0 \le E(t) \le E^{max}. \tag{4.4}$$

The Hamiltonian corresponding to this optimisation problem is given by

$$\begin{aligned} H = e^{-\xi t} &\left[\frac{p_1 qErKx}{m_1\mu Ee^{\mu\tau} + K\{m_1\rho E(e^{\mu\tau} - 1) + m_2\mu\}x} \right] \\ &+ \epsilon \left[x(1-x) - \frac{\alpha xy}{\sigma x + \gamma y + c} - \frac{qErKx}{m_1\mu Ee^{\mu\tau} + K\{m_1\rho E(e^{\mu\tau} - 1) + m_2\mu\}x} \right], \end{aligned} \tag{4.5}$$

where ϵ is the adjoint variable. Differentiating the Hamiltonian with respect to E gives

$$\frac{\partial H}{\partial E} = (e^{-\xi t}p_1 - \epsilon)\frac{m_2K^2p_1qrx^2}{[m_1\mu Ee^{\mu\tau} + K\{m_1\rho E(e^{\mu\tau}-1)+m_2\mu\}x]^2} = \sigma(t). \tag{4.6}$$

The optimal control $E(t)$ must satisfy the following

$$E(t) = \begin{cases} E^{max}, & \text{if } \sigma(t) > 0, \\ 0, & \text{if } \sigma(t) < 0, \end{cases}$$

where $\sigma(t)$ is the switching function that drives $E(t)$ between the bounds 0 and E^{max}, resulting in a bang-bang control.

When $\sigma(t) = 0$, the Hamiltonian does not depend on $E(t)$ directly; thus, the control is unique and satisfies $0 < E^*(t) < E^{max}$ for all E. Therefore, the optimal harvesting strategy is

$$E(t) = \begin{cases} E^{max}, & \text{if } \sigma(t) > 0, \\ 0, & \text{if } \sigma(t) < 0, \\ E^*, & \text{if } \sigma(t) = 0. \end{cases}$$

For $\sigma(t) = 0$, we have from (4.6)

$$\epsilon = e^{-\xi t}\left(p_1 - \frac{[m_1\mu Ee^{\mu\tau} + K\{m_1\rho E(e^{\mu\tau}-1)+m_2\mu\}x]^2}{m_2K^2p_1qrx^2}\right). \tag{4.7}$$

According to Pontryagin's maximum principle [16], the adjoint equation is

$$\frac{d\epsilon}{dt} = -\frac{\partial H}{\partial x}. \tag{4.8}$$

Substituting from (4.5), we obtain

$$\begin{aligned}\frac{d\epsilon}{dt} &= -\frac{e^{-\xi t}m_1\mu E^2qrKp_1e^{\mu\tau}}{[m_1\rho E(e^{\mu\tau}-1)+m_2\mu\}x]^2} \\ &\quad - \epsilon\left[1 - 2x - \frac{\alpha\gamma y^2 + c\alpha y}{(\sigma x+\gamma y+c)^2} - \frac{m_1\mu E^2qrKe^{\mu\tau}}{[m_1\mu Ee^{\mu\tau} + K\{m_1\rho E(e^{\mu\tau}-1)+m_2\mu\}x]^2}\right].\end{aligned} \tag{4.9}$$

At equilibrium, (4.9) reduces to

$$\begin{aligned}\frac{d\epsilon}{dt} &= -\frac{e^{-\xi t}m_1\mu E^2qrKp_1e^{\mu\tau}}{[m_1\rho E(e^{\mu\tau}-1)+m_2\mu\}x]^2} \\ &\quad - \epsilon\left[-x - \frac{\alpha\gamma y^2 + c\alpha y}{(\sigma x+\gamma y+c)^2} + \frac{qErK^2(m_1\rho E(e^{\mu t}-1)+m_2)}{[m_1\mu Ee^{\mu\tau} + K\{m_1\rho E(e^{\mu\tau}-1)+m_2\mu\}x]^2}\right].\end{aligned} \tag{4.10}$$

Using the value of ϵ from (4.7) in (4.10), we get

$$\begin{aligned}\frac{d\epsilon}{dt} &= -\frac{e^{-\xi t}m_1\mu E^2qrKp_1e^{\mu t}}{[m_1\rho E(e^{\mu\tau}-1)+m_2\mu\}x]^2} \\ &\quad - e^{-\xi t}\left(p_1 - \frac{c_2[m_1\rho E(e^{\mu\tau}-1)+m_2\mu\}x]^2}{m_2K^2p_1qrx^2}\right) \\ &\quad \times\left[-x - \frac{\alpha\gamma y^2 + c\alpha y}{(\sigma x+\gamma y+c)^2} + \frac{qErK^2(m_1\rho E(e^{\mu t}-1)+m_2)}{[m_1\mu Ee^{\mu\tau} + K\{m_1\rho E(e^{\mu\tau}-1)+m_2\mu\}x]^2}\right].\end{aligned} \tag{4.11}$$

Integrating (4.11) gives

$$\begin{aligned}\epsilon = \frac{1}{\xi}e^{-\xi t}[\ &\frac{m_1\mu E^2qrKp_1e^{\mu t}}{[m_1\rho E(e^{\mu\tau}-1)+m_2\mu\}x]^2} + (p_1 - \frac{c_2[m_1\rho E(e^{\mu\tau}-1)+m_2\mu\}x]^2}{m_2K^2p_1qrx^2}) \\ &\times(-x - \frac{\alpha\gamma y^2 + c\alpha y}{(\sigma x+\gamma y+c)^2} + \frac{qErK^2(m_1\rho E(e^{\mu t}-1)+m_2)}{[m_1\mu Ee^{\mu\tau+Km_1\rho E(e^{\mu\tau}-1)+m_2\mu}x]^2})]\end{aligned} \tag{4.12}$$

The term $\epsilon e^{\xi t}$ represents the shadow price of the prey population—i.e., the implicit economic value of unmeasured costs. To maintain the shadow price at minimal levels, we disregard the integration constant.

From (4.7) and (4.12), we derive

$$\begin{aligned}\left(p_1 - \frac{c_2[m_1\rho E(e^{\mu\tau}-1)+m_2\mu\}x]^2}{m_2K^2p_1qrx^2}\right) = \frac{1}{\xi}\Bigg[&\frac{m_1\mu E^2qrKp_1e^{\mu t}}{[m_1\rho E(e^{\mu\tau}-1)+m_2\mu\}x]^2}\\ &+\left(p_1 - \frac{c_2[m_1\rho E(e^{\mu\tau}-1)+m_2\mu\}x]^2}{m_2K^2p_1qrx^2}\right)\\ &\times\left(-x - \frac{\alpha\gamma y^2+c\alpha y}{(\sigma x+\gamma y+c)^2}\right.\\ &\left.+\frac{qErK^2(m_1\rho E(e^{\mu t}-1)+m_2)}{[m_1\mu Ee^{\mu\tau}+K\{m_1\rho E(e^{\mu\tau}-1)+m_2\mu\}x]^2}\right)\Bigg].\end{aligned} \tag{4.13}$$

The optimal solution (x_τ, y_τ) and optimal harvesting effort E_τ are obtained by solving the steady state system together with Eq. (4.13). The optimal effort, denoted by E^{Opt}, corresponds to the unique positive real solution of Eq. (4.13).

5. Sensitivity Analysis

Sensitivity analysis provides valuable information about the manner in which small perturbations in parameters influence the dynamical behaviour of a system. This type of analysis is especially important for delay differential models, where parameters may play different roles in instantaneous and delayed interactions. In this section, we derive first-order sensitivity equations for the predator-prey system

$$\frac{dx}{dt} = x(1-x) - \frac{\alpha xy}{\sigma x+\gamma y+c} - \frac{h\,x(t-\tau)}{c_1+x(t-\tau)}, \tag{5.1a}$$

$$\frac{dy}{dt} = \delta\, y\left(1-\frac{\beta y}{x}\right), \tag{5.1b}$$

where h, c_1, and τ denote, respectively, the harvesting rate, the saturation parameter and the maturity delay in the prey population. For convenience, we denote the delayed prey density by $x_\tau(t) = x(t-\tau)$.

Sensitivity functions. Let ρ represent any scalar parameter of the model (e.g. $\rho \in \{h, c_1, \tau\}$). The sensitivity of the solution with respect to ρ is defined by

$$S_{x,\rho}(t) = \frac{\partial x(t)}{\partial \rho}, \qquad S_{y,\rho}(t) = \frac{\partial y(t)}{\partial \rho}.$$

To derive governing equations for these functions, we differentiate the right-hand sides of (5.1a) - (5.1b) with respect to ρ.

We introduce the notation

$$F_1(x,y,x_\tau) = x(1-x) - \frac{\alpha xy}{\sigma x+\gamma y+c} - \frac{h\,x_\tau}{c_1+x_\tau}, \qquad F_2(x,y) = \delta y\Big(1-\frac{\beta y}{x}\Big).$$

Differentiating (5.1a) - (5.1b) yields

$$\frac{dS_{x,\rho}}{dt} = F_{1x}\,S_{x,\rho} + F_{1y}\,S_{y,\rho} + F_{1x_\tau}\,S_{x,\rho}(t-\tau) + F_{1\rho}, \tag{5.2a}$$

$$\frac{dS_{y,\rho}}{dt} = F_{2x}\,S_{x,\rho} + F_{2y}\,S_{y,\rho} + F_{2\rho}. \tag{5.2b}$$

The partial derivatives in (5.2) are computed along the nominal solution $(x(t), y(t))$:

$$F_{1x} = (1-2x) - \alpha y \frac{(\sigma x + \gamma y + c) - \sigma x}{(\sigma x + \gamma y + c)^2}, \quad F_{1y} = -\alpha x \frac{(\sigma x + \gamma y + c) - \gamma y}{(\sigma x + \gamma y + c)^2},$$

$$F_{1x_\tau} = -h\,\frac{c_1}{(c_1 + x_\tau)^2}, \quad F_{2x} = \delta\, y\, \frac{\beta y}{x^2}, \quad F_{2y} = \delta\left(1 - 2\beta\frac{y}{x}\right).$$

Sensitivity with respect to the harvesting parameter h. The only explicit dependence of F_1 on h is through the delayed term. Hence

$$F_{1h} = -\frac{x_\tau}{c_1 + x_\tau}, \qquad F_{2h} = 0.$$

Substituting these into (5.2) gives

$$\frac{dS_{x,h}}{dt} = F_{1x}\, S_{x,h} + F_{1y}\, S_{y,h} + F_{1x_\tau}\, S_{x,h}(t-\tau) - \frac{x_\tau}{c_1 + x_\tau}, \tag{5.3a}$$

$$\frac{dS_{y,h}}{dt} = F_{2x}\, S_{x,h} + F_{2y}\, S_{y,h}. \tag{5.3b}$$

Sensitivity with respect to the saturation parameter c_1. Differentiating the term $-\dfrac{hx_\tau}{c_1 + x_\tau}$ gives

$$F_{1c_1} = \frac{hx_\tau}{(c_1 + x_\tau)^2}, \qquad F_{2c_1} = 0.$$

Thus, the c_1 sensitivity equations are

$$\frac{dS_{x,c_1}}{dt} = F_{1x}\, S_{x,c_1} + F_{1y}\, S_{y,c_1} + F_{1x_\tau}\, S_{x,c_1}(t-\tau) + \frac{hx_\tau}{(c_1 + x_\tau)^2}, \tag{5.4a}$$

$$\frac{dS_{y,c_1}}{dt} = F_{2x}\, S_{x,c_1} + F_{2y}\, S_{y,c_1}. \tag{5.4b}$$

Sensitivity with respect to the delay parameter τ. Sensitivity with respect to the delay requires special treatment because

$$\frac{\partial x(t-\tau)}{\partial \tau} = -\,x'(t-\tau) - S_{x,\tau}(t-\tau).$$

Hence

$$F_{1\tau} = F_{1x_\tau}\frac{\partial x_\tau}{\partial \tau} = -h\frac{c_1}{(c_1 + x_\tau)^2}\left[x'(t-\tau) + S_{x,\tau}(t-\tau)\right].$$

Substituting this expression into (5.2) yields a neutral delay system:

$$\frac{dS_{x,\tau}}{dt} = F_{1x}\, S_{x,\tau} + F_{1y}\, S_{y,\tau} + F_{1x_\tau}\Big(S_{x,\tau}(t-\tau) - x'(t-\tau)\Big), \tag{5.5a}$$

$$\frac{dS_{y,\tau}}{dt} = F_{2x}\, S_{x,\tau} + F_{2y}\, S_{y,\tau}. \tag{5.5b}$$

Because no parameter perturbation is imposed before $t = 0$, the sensitivity functions satisfy.

$$S_{x,\rho}(t) = 0, \qquad S_{y,\rho}(t) = 0, \qquad t \in [-\tau, 0],$$

for all parameters $\rho \in \{h, c_1, \tau\}$.

The local sensitivity of the delayed predator-prey system (5.1) with respect to the parameters h, c_1, and τ is described by the combined system consisting of the original model together with the associated delay or neutral-delay sensitivity equations (5.3), (5.4), and (5.5). These equations quantify the first-order response of the state variables to infinitesimal changes in the parameters and provide a mathematical basis for assessing model robustness and parameter influence. sectionNumerical simulation The stability results of model system (2.5) for the different parameter value sets are

provided below.
The Figure 1, and Figure 3 (when $\tau = 0$), the parametric values are $\alpha = 0.381, \sigma = 0.26, \gamma = 0.45, c = 0.681, h = 0.186, c_1 = 0.326, \delta = 0.783, \beta = 0.275$, $(0.2536211309, 0.9222586579)$ for the system (2.5). Figures 1 and 3 denote the basin of attraction; red, yellow, and blue represent the unstable, saddle, and stable regions, respectively. In Figures 1 and 3 of the system (2.5) and non-delay system when $\tau = 0$, respectively, if the values of beta increase, then the saddle region portion decreases and the stable region increases.
When delay is incorporated into the model (2.5) with $\tau = 0.5$ (black dashed line) and $\tau = 7.5$ (red dashed line), as shown in Figure 4, using the parameter values listed in Table 2, it is observed that these parameter sets satisfy the conditions for both the limit cycle and the absolute stability of the coexistence equilibrium point. Figure 4a, 4c, and 4e shows that the system is stable, whereas Figure 4b, 4d, and 4f shows that the system is unstable.

TABLE 2. Interior Steady Point with its nature for Figure 4.

Non-negative variables	Steady Point	Nature	Fig No.
$\alpha = 0.381, \sigma = 0.26, \gamma = 0.45, c = 0.681, h = 0.186, c_1 = 0.326, \delta = 0.783, \beta = 0.275$	$(0.2536211309, 0.9222586579)$	Stable	4a
$\alpha = 0.981, \sigma = 0.16, \gamma = 0.485, c = 0.681, h = 0.781, c_1 = 0.426, \delta = 0.183, \beta = 0.375$	$(2.737800216, 7.300800576)$	Unstable	4b
$\alpha = 0.981, \sigma = 0.16, \gamma = 0.485c = 0.681, h = 0.186, c_1 = 0.326, \delta = 0.783, \beta = 0.3475$	$(0.1321454899, 0.3802747910)$	stable	4c
$\alpha = 0.981, \sigma = 0.16, \gamma = 0.485, c = 0.681, h = 0.618, c_1 = 0.426, \delta = 0.283, \beta = 0.475$	$(2.539031258, 5.345328964)$	Unstable	4d
$\alpha = 0.981, \sigma = 0.26, \gamma = 0.45, c = 0.681, h = 0.186, c_1 = 0.326, \delta = 0.783, \beta = 0.275$	$(0.1140214445, 0.4146234347)$	Stable	4e
$\alpha = 0.81, \sigma = 0.1, \gamma = 0.485, c = 0.2, h = 0.918, c_1 = 0.426, \delta = 0.283, \beta = 0.75$	$(2.367272720, 3.156363627)$	Unstable	4f

In Figure 5, the phase portrait of the systems (2.5) and when $\tau = 0$. If we increase the values of τ, the limit cycle is stable.

Figures 6 and 7 illustrate the bifurcation structure and Hopf bifurcation curves in the (x, y) plane for varying parameters at $\tau = 0.5$. The computations are carried out using the parameter values $\sigma = 0.26$, $\gamma = 0.45$, $\alpha = 0.381$, $c = 0.681$, $h = 0.186$, $c_1 = 0.326$, $\delta = 0.783$, and $\beta = 0.275$, with the interior equilibrium point located at (0.2536211309, 0.9222586579). The figure reveals the presence of several bifurcation phenomena, including Hopf bifurcation (H), limit points (LP), period-doubling bifurcation (PD), and limit point cycles (LPC), which characterise the transitions in system dynamics. The stable equilibrium point (EP) curves are shown in black, while the unstable EP curves are depicted in green, as illustrated in parts 6a, 6b, and 7a, 7b. In the Hopf bifurcation parts 6c, and 7c, the stable regions are indicated in green and the unstable regions in blue. Overall, the figure demonstrates how

variations in the parameters influence the stability of the equilibrium and give rise to oscillatory and complex dynamical behaviour.

Figure 8 illustrates the Hopf bifurcation behaviour of the prey - predator system with respect to the parameters h, c_1, and the time delay τ. The diagrams show the transition between equilibrium and oscillatory dynamics under variations of the key system parameters. For Figures 8a and 8b, the parameter values are chosen as $\alpha = 0.8, \quad \sigma = 0.5, \quad \gamma = 0.2, \quad c = 0.1, \quad \beta = 2.0, \quad \delta = 0.05, \quad \tau = 0.94, \quad c_1 = 0.8$, while the bifurcation parameter h varies in the interval $0 \leq h \leq 0.8$ with a step size of 0.001. As h increases, the coexistence equilibrium loses stability through a Hopf bifurcation, giving rise to sustained periodic oscillations in the prey population. A further increase in h enlarges the oscillation amplitude, indicating the emergence of more complex dynamical behaviour. For Figures 8c and 8d, the parameters are fixed as $\alpha = 0.8, \quad \sigma = 0.5, \quad \gamma = 0.2, \quad c = 0.1, \quad \beta = 2.15, \quad \delta = 0.05, \quad \tau = 0.94, \quad h = 0.786$, and the parameter c_1 varies over the range $0.7 \leq c_1 \leq 2$ with a step size of 0.001. The bifurcation diagram shows a transition from chaotic oscillations to periodic solutions and finally to a stable coexistence equilibrium. This behaviour indicates that increasing c_1 has a stabilising effect on the prey-predator dynamics through a process of periodic halving. For Figures 8e and 8f, the bifurcation with respect to the delay parameter τ is presented by choosing $\alpha = 0.9, \quad \sigma = 0.5, \quad \gamma = 0.7, \quad c = 0.21, \quad \beta = 2.15, \quad \delta = 0.05, \quad c_1 = 0.9, \quad h = 0.786$, while τ varies in the interval $0.1 \leq \tau \leq 1.2$ with a step size of 0.001. For small values of τ, the system admits a stable equilibrium. When τ exceeds a critical value, a Hopf bifurcation occurs, and periodic oscillations emerge. Further increases in τ lead to amplitude growth and complex dynamics, indicating a transition toward chaotic behaviour. Furthermore, the Hopf bifurcation diagrams reveal that variations in h and τ drive the system from a stable equilibrium to periodic and chaotic oscillations via period-doubling, whereas changes in c_1 lead to a reverse transition from chaotic dynamics to stable coexistence through periodic halving. These results emphasise the significant role of harvesting intensity, interaction strength, and time delay in governing the long-term dynamics of the prey - predator system. With the parameter values $\alpha = 0.01 \quad \sigma = 0.1 \quad \gamma = 2.461 \quad c = 0.549 \quad c_1 = 0.4869 \quad \delta = 0.75 \quad \beta = 0.0001$ and harvesting effort $E \in [0, 1]$, Figure 9a illustrates the relationship between the yield Y and the harvest rate h for system (2.5) at different values of the delay parameter τ. In all cases, the yield initially increases with the harvest rate, reaches a maximum value, and then decreases as the harvesting pressure continues to increase. As the delay parameter τ increases, the peak yield shifts toward lower harvest rates and the decline beyond the maximum becomes steeper. This behaviour indicates that stronger delay effects reduce the range of sustainable harvesting and limit the system's ability to tolerate high harvest rates.

For Figure 9b, the parameters are chosen as $\alpha = 3.958 \quad \sigma = 3.956 \quad \gamma = 0.421 \quad c = 0.256 \quad h \in [0, 1000] \quad c_1 = 2.958 \quad \delta = 0.465 \quad \beta = 0.935$. This figure depicts the yield-harvest relationship for system (2.5) under different values of c_1. The results show that an increase in c_1 leads to a higher maximum sustainable yield (MSY) and shifts the optimal harvest rate h^* toward larger values. The marked points on the curves represent the MSY and the corresponding optimal harvesting levels. These results suggest that larger values of c_1 enhance the system's capacity to sustain higher yields under harvesting.

With this set of parameters, we observe the typical variation of net revenue R(or economic rent) over time as $\tau \in [0, 10]$ with a constant harvesting effort $E = 0.1$ at any time $t > \tau$. Prey harvesting is considered profitable when the prey density and cost per unit effort satisfy the conditions $(x, c) = (10, 0.2)$ and $(x, \bar{c}) = (50, 0.2)$, as shown in Figures 10a and 10c. Conversely, harvesting is not profitable when $(x, \bar{c}) = (50, 0.5)$, $(x, c) = (500, 0.5)$, as depicted in Figures 10b and 10d. The fluctuations in economic rent or net revenue R with respect to $\tau \in [0, 10]]$ are clearly shown, with lines in Figures 10b and 10d indicating un-profitability of prey harvesting, while lines in Figures 10a and 10c indicate profitability.

In Figure 11, the parameter values are chosen as $\alpha = 0.9, \quad \sigma = 0.4, \quad \gamma = 0.3, \quad c = 0.5, \quad \delta = 0.6, \quad \beta = 0.75, \quad h = 0.2, \quad c_1 = 0.8, \quad \tau = 11.5$, with the initial condition $(0.2536211309, \ 0.9222586579)$. Table 3 summarises the numerical sensitivity analysis of the state variables with respect to the parameters h, c_1, and τ. The table reports the maximum absolute sensitivity, mean absolute sensitivity, and the final sensitivity value. The results indicate that the system is most sensitive to variations in the parameter h, followed by c_1, whereas the sensitivities associated with τ are comparatively small. This suggests that changes in h have a stronger impact on the system dynamics than

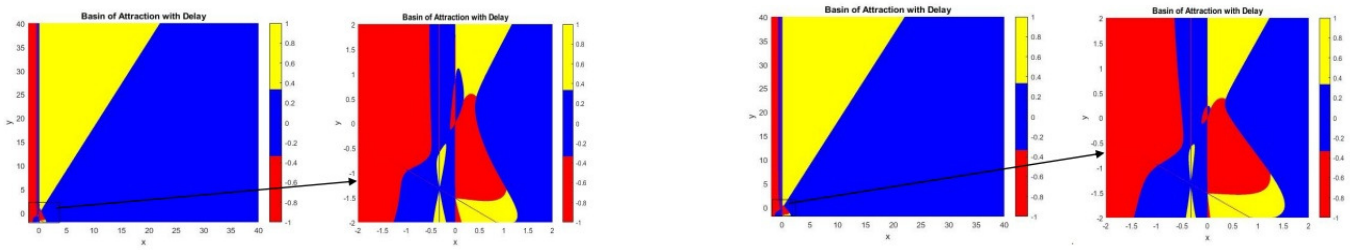

(A) (B)

FIGURE 1. Bassin of attraction for system's (2.5).

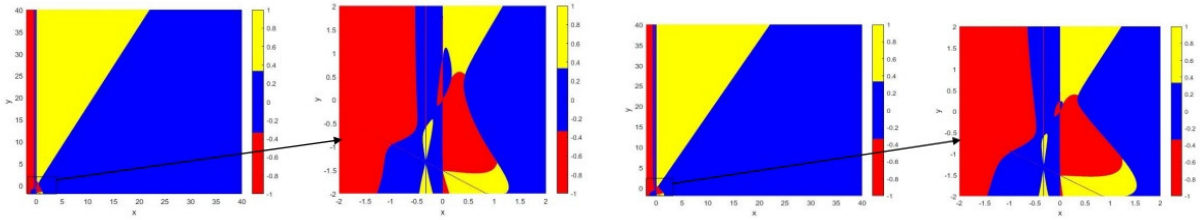

(A) (B)

FIGURE 2. Bassin of attraction for system when $\tau = 0$ as non-delay.

FIGURE 3

TABLE 3. Numerical Sensitivity Summary of prey and predator populations with respect to the harvesting rate h, saturation parameter c_1, and delay τ.

	$S_{x,h}$	$S_{y,h}$	S_{x,c_1}	S_{y,c_1}	$S_{x,\tau}$	$S_{y,\tau}$
Max $\|S\|$	0.77706	0.91057	0.14750	0.17285	0.0085327	0.0090822
Mean $\|S\|$	0.47164	0.62384	0.085004	0.11248	0.0009617	0.0010871
Final value	-0.47284	-0.63061	0.084672	0.11292	-1.8438e-05	-1.4084e-05

variations in c_1 and τ.

6. Summary and Conclusion

This paper investigates a two-species Leslie-Gower type predator-prey model incorporating a Beddington-DeAngelis functional response, non-linear prey harvesting, and a maturation delay. A comprehensive analytical and numerical study is carried out for the delayed system (2.5) using bifurcation theory, stability analysis, optimal harvesting strategies, bionomic equilibrium, sustainable yield, and maximum sustainable yield (MSY) policies.

The yield-harvest relationship for the model system (2.5) is examined in detail, and the corresponding yield-effort curves reveal the existence of an optimal harvesting rate that maximises sustainable yield. Table 2 classifies the interior equilibrium points as stable or unstable for different parameter sets, thereby distinguishing coexistence equilibria from oscillatory regimes. The non-delayed system is interpreted through the ratio of the harvesting rate constant h to the intrinsic growth rates of the prey and predator populations, consistent with the approach reported by Zhang et al. [30].

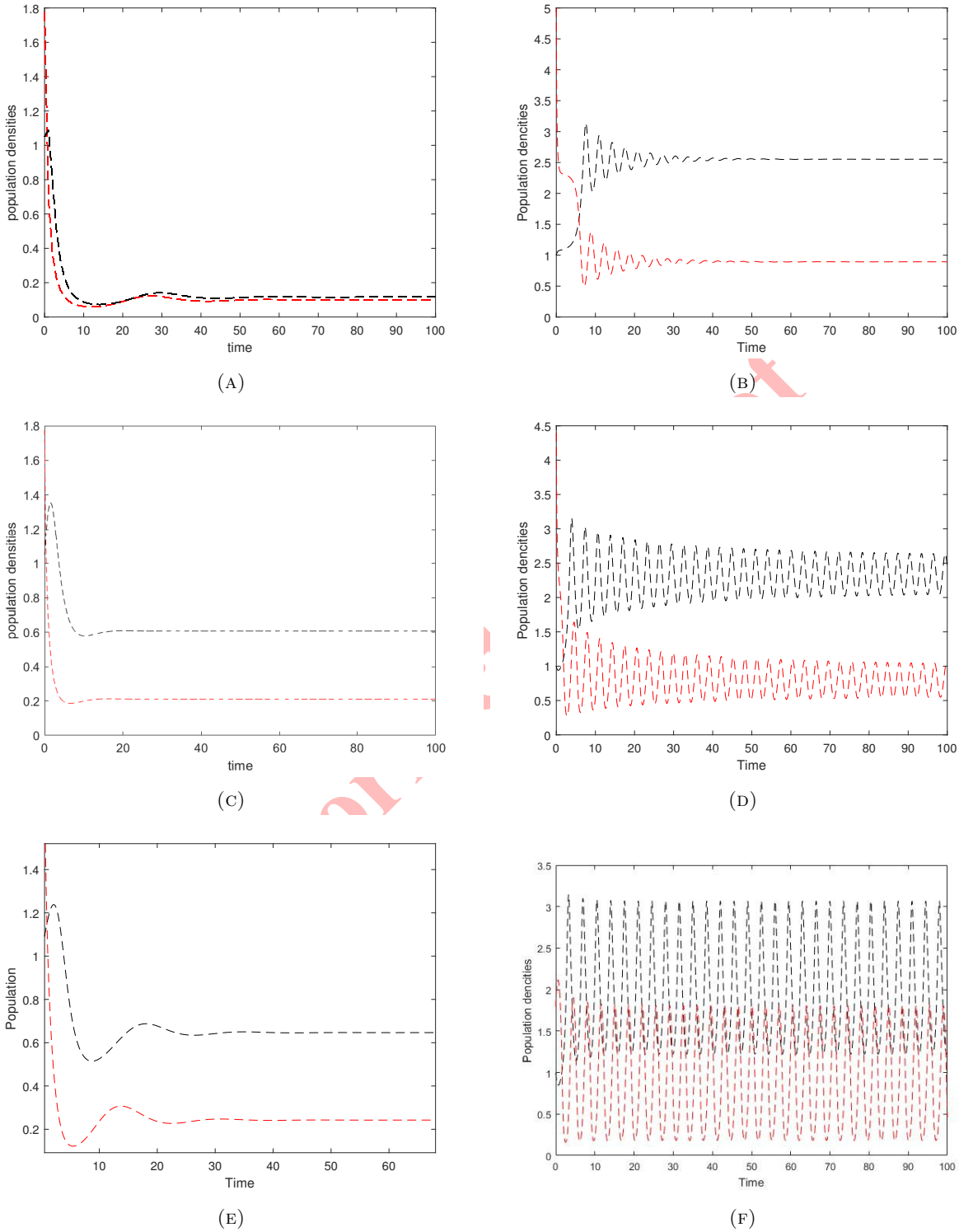

FIGURE 4. The time series solution of the system (2.5) is presented for various initial values and parameters, with $\tau = 0.5$(black dashed line) and $\tau = 7.5$ (red dashed line) for comparison.

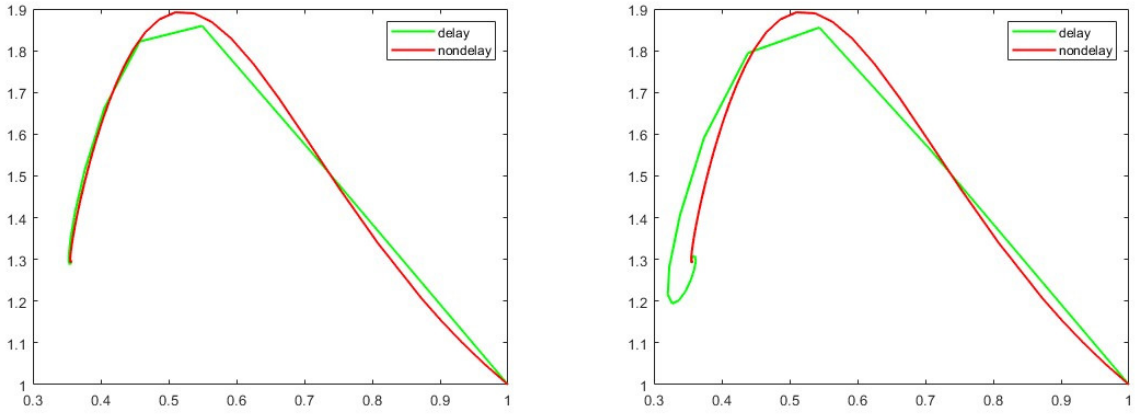

(A) $\tau = 1$.

(B) $\tau = 3$.

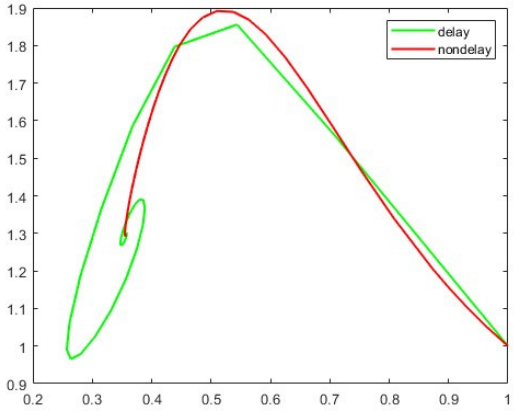

(C) $\tau = 5$.

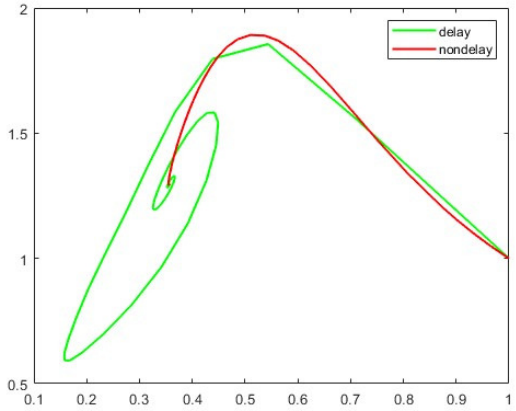

(D) $\tau = 7$.

FIGURE 5. Phase portrait of the system's (2.5) and when non-delay such as $\tau = 0$ (see[1]).

The analytical results demonstrate that the system undergoes a Hopf bifurcation around the coexistence equilibrium, leading to the emergence of stable limit cycles. In addition, saddle-node bifurcations are observed near critical values of the control parameters, indicating sudden qualitative changes in population dynamics. The inclusion of time delay significantly enriches the system dynamics, promoting oscillatory behaviour, and, for larger delays, complex and chaotic fluctuations [27, 31].

To explore optimal harvesting policies, a suitable Hamiltonian function is constructed, and the Pontryagin maximum principle is applied to derive the optimal control strategy. The results indicate that the harvesting effort plays a dominant role in regulating population stability and economic returns, while excessive delay reduces the sustainable harvesting range. These findings highlight the trade-off between ecological stability and economic profit in harvested ecosystems.

The present results are consistent with recent studies on delayed predator-prey systems with non-linear harvesting. In particular, the spatial extension of the model (2.5) analysed by Upadhyay et al. [26] revealed the direction and stability of Hopf bifurcations and demonstrated the emergence of Turing patterns under non-linear harvesting. Such spatial patterns, including spots and stripes, are known to improve predator survival, facilitate social communication,

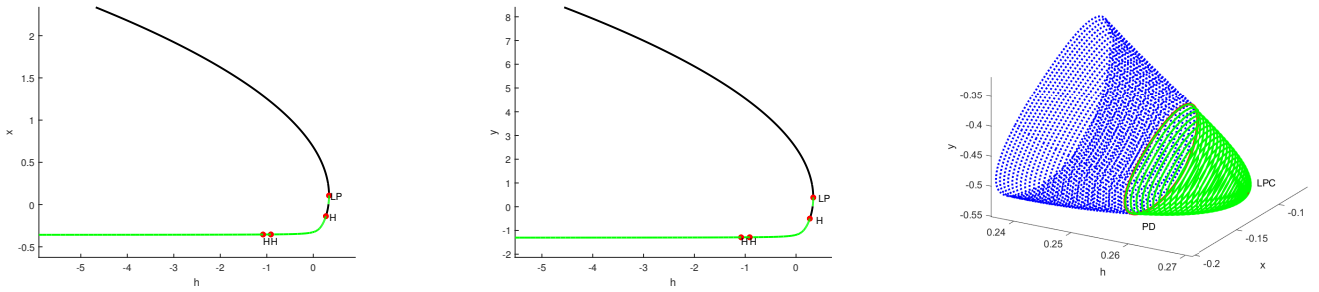

(A) (B) (C)

FIGURE 6. When $\tau = 0.5$, bifurcation and Hopf bifurcation diagrams are shown among x, y, and h.

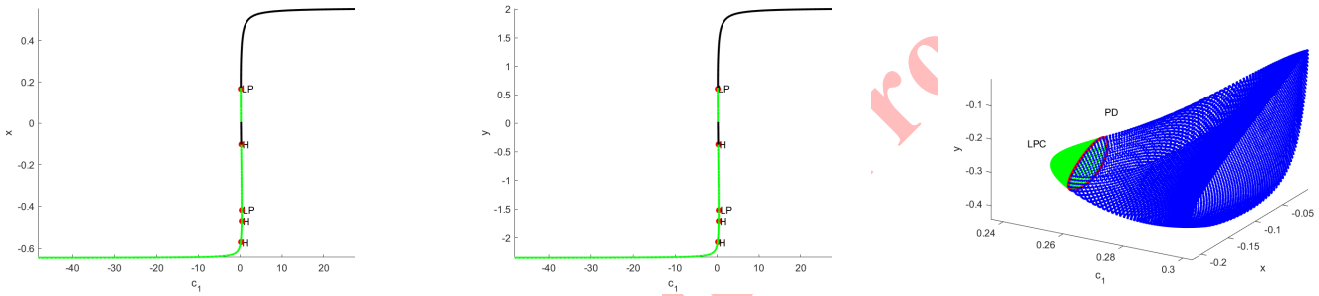

(A) (B) (C)

FIGURE 7. When $\tau = 0.5$, bifurcation and Hopf bifurcation diagrams are shown among x, y, and c_1.

and improve defence mechanisms, thereby supporting long-term persistence of species [13].
Furthermore, the combined numerical and theoretical results confirm that harvesting intensity, saturation effects, and maturation delay are key drivers of prey-predator dynamics. The model provides valuable insights into sustainable resource management and offers a flexible framework for studying ecological systems subject to harvesting, time delay, and environmental feedback.
The present study can be extended in several directions to improve its ecological realism and analytical scope. One possible extension is the inclusion of environmental stochasticity to represent random variations in climate, resource availability, and harvesting intensity. This would help assess the robustness of stability and bifurcation outcomes under uncertain ecological conditions. Another important direction is the incorporation of spatial diffusion, which would allow the investigation of spatio-temporal dynamics and pattern formation in heterogeneous environments. Future work may also explore alternative functional responses, such as ratio-dependent or Holling-type forms with predator interference, to better understand how interaction mechanisms affect system stability and harvesting outcomes. In addition, introducing stage structure in prey and predator populations could provide insights into maturation effects and age-dependent harvesting strategies. From a management perspective, time-dependent harvesting and adaptive control policies may be considered to balance long-term economic benefits with ecological sustainability.

Acknowledgement. Dr. Jyotiska Datta: Conceptualisation.
Mr Atish Kumar Sethy: Mathematical Derivation and Numerical Simulation.

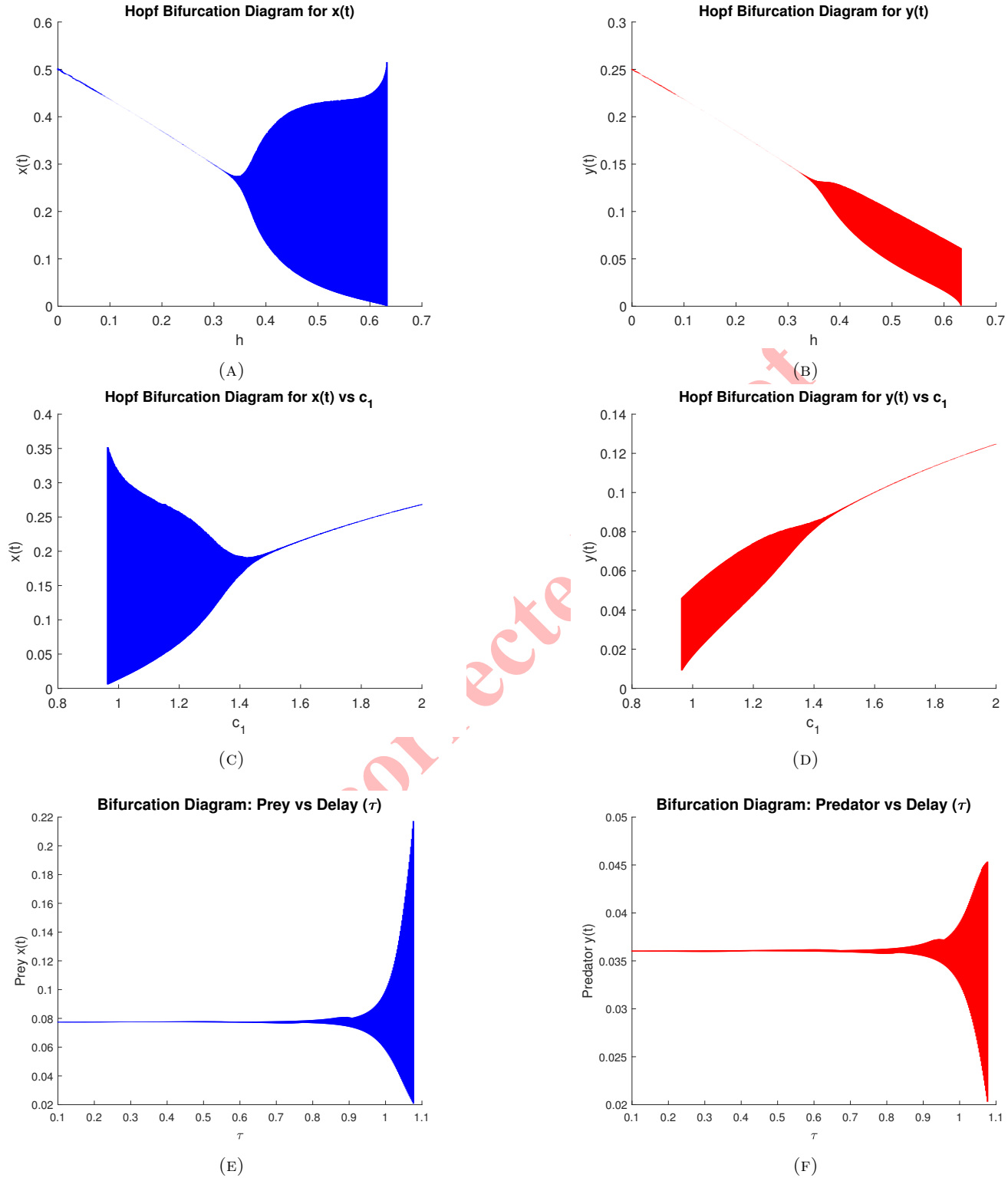

FIGURE 8. Bifurcation diagram between h, c_1, τ vs prey and predator populations.

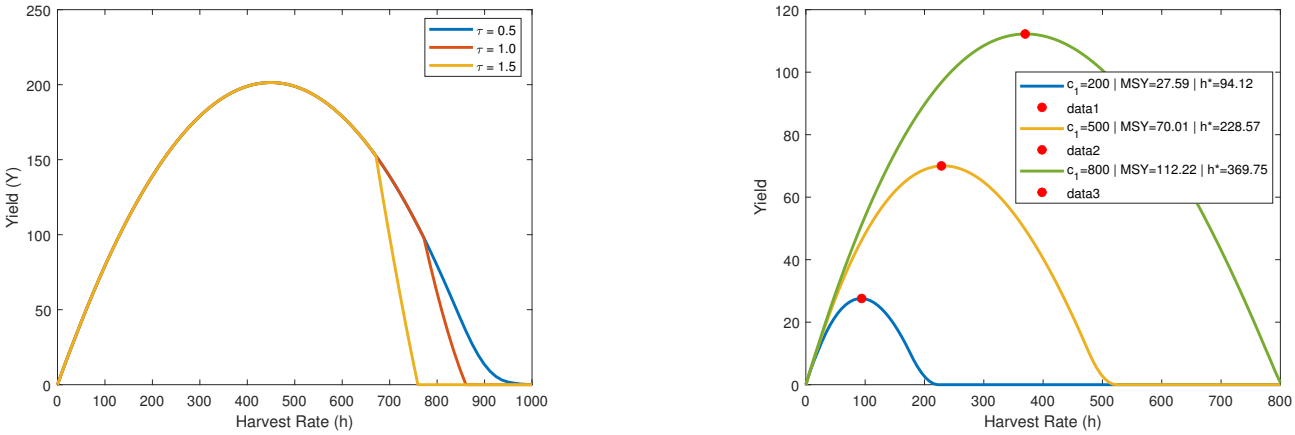

(A) (B)

FIGURE 9. Graph of system yield-effort for figure (a) and Harvest rate- MSY for figure (b) of system (2.5). In the text, the parameter set is provided.

REFERENCES

[1] H. J. Alsakaji, S. Kundu, and F. A. Rihan, *Delay differential model of one-predator two-prey system with Monod-Haldane and Holling type II functional responses*, Appl. Math. Comput., *397* (2021), 125919.

[2] D. Alonso and R. V. Solé, *Delay effects and resilience in ecological networks*, Nat. Ecol. Evol., *8* (2025), 312–320.

[3] J. Arino, L. Wang, and G. S. K. Wolkowicz, *An alternative formulation for a delayed logistic equation*, J. Theor. Biol., *241* (2006), 109–119.

[4] J. Arino, L. Wang, and G. S. K. Wolkowicz, *An alternative formulation for a delayed logistic equation*, J. Theor. Biol., *241* (2006), 109–119.

[5] T. K. Banerjee, U. S. Hazra, and R. Banerjee, *Studies on the incidence behavior and morphometry of Hilsa fish, Tenualosa ilisha in relation to environmental attributes in the selected portion of the upper stretch of Hooghly estuary*, Springer, *1* (2013), 226–247.

[6] Y. Chen and G. Sun, *Spatiotemporal dynamics and Turing patterns in predator-prey systems with harvesting*, Ecol. Complexity, *55* (2023), 101159.

[7] K. L. Cooke and P. van den Driessche, *On zeroes of some transcendental equations*, Funkcial. Ekvac., *29* (1986), 77–90.

[8] J. Datta, A. K. Sethy, and R. K. Upadhyay, *Understanding the spatiotemporal dynamics and pattern analysis of population model with Holling type-IV functional response*, Pramana - J. Phys., *100* (2026), 69.

[9] B. Ghosh and S. Banerjee, *Economic and ecological trade-offs in harvested predator-prey models*, Ecol. Modell., *492* (2024), 110770.

[10] R. Agrawal, D. Jana, R. K. Upadhyay, and V. S. H. Rao, *Complex dynamics of sexually reproductive generalist predator and gestation delay in a food chain model: double Hopf-bifurcation to chaos*, J. Appl. Math. Comput., *55*(1–2) (2017), 513–547.

[11] D. Jana, R. Agrawal, R. K. Upadhyay, and G. P. Samanta, *Ecological dynamics of age selective harvesting of fish population: maximum sustainable yield and its control strategy*, Chaos Solitons Fractals, *93* (2016), 1–11.

[12] D. Jana, R. Pathak, and M. Agarwal, *On the stability and Hopf bifurcation of a prey-generalist predator system with independent age-selective harvesting*, Chaos Solitons Fractals, *83* (2016), 252–273.

[13] J. L. Kelley, J. L. Fitzpatrick, and S. Merilaita, *Spots and stripes: ecology and colour pattern evolution in butterflyfishes*, Proc. R. Soc. B, *280*(1757) (2013), 20122730.

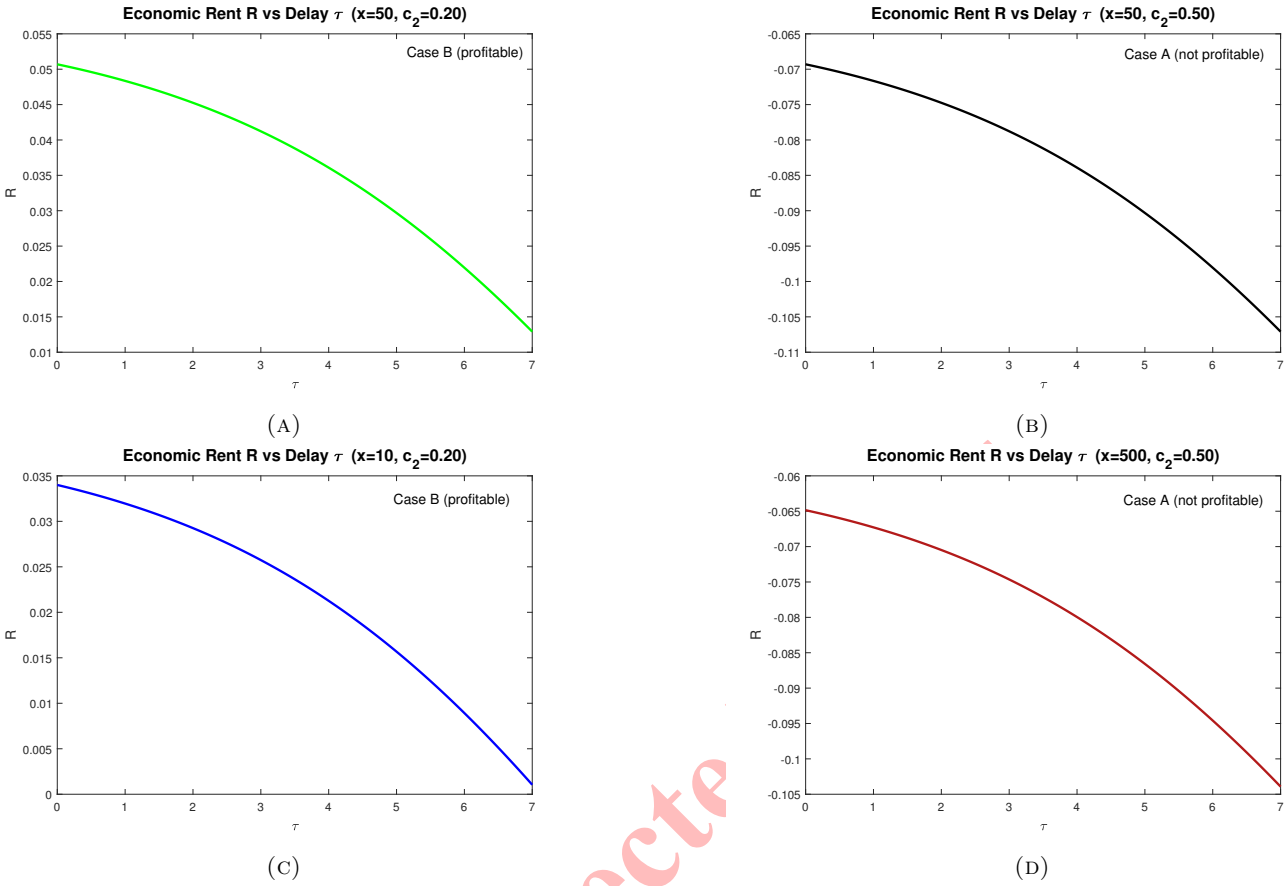

FIGURE 10. With a constant harvesting effort $E = 0.1$, the prey density and cost per unit effort are set as follows: $(x, \bar{c})$: $(50, 0.2)$, $(50, 0.5)$, $(10, 0.2)$, $(500, 0.5)$ for figures (a)–(d), respectively.

[14] A. Kumar and M. Singh, *Bifurcation and chaos control in predator-prey systems with harvesting*, J. Biol. Dyn., *18* (2024), 145–164.

[15] H. Li and J. Zhao, *Optimal harvesting strategies in delayed bioeconomic predator-prey models*, Appl. Math. Modell., *123* (2024), 265–283.

[16] L. S. Pontryagin, V. S. Boltyonskii, R. V. Gamkrelidze, and E. F. Mishchenko, *The mathematical theory of optimal process*, Wiley, New York, 1962.

[17] M. Rahman and J. Chattopadhyay, *Delay-induced instability and stabilization in predator-prey systems*, Math. Comput. Simul., *215* (2023), 29–47.

[18] S. Rashi, U. K. Suruchi, S. P. Anuj, H. Harendra, and S. K. Prashant, *Cooperation and harvesting-induced delays in a predator-prey model with prey fear response: a crossing curves approach*, Chaos Solitons Fractals, *2025* (2025), 116132.

[19] J. D. Reynolds, *A review of ecological interactions between crayfish and fish, indigenous and introduced*, Knowl. Manage. Aquat. Ecosyst., *401* (2011), 10.

[20] F. A. Rihan, *Delay differential equations and applications to biology*, Springer, Singapore, 2021.

[21] F. A. Rihan, H. J. Alsakaji, and C. Rajivganthi, *Stability and Hopf bifurcation of three-species prey-predator system with time delays and Allee effect*, Complexity, *2020* (2020), 7306412.

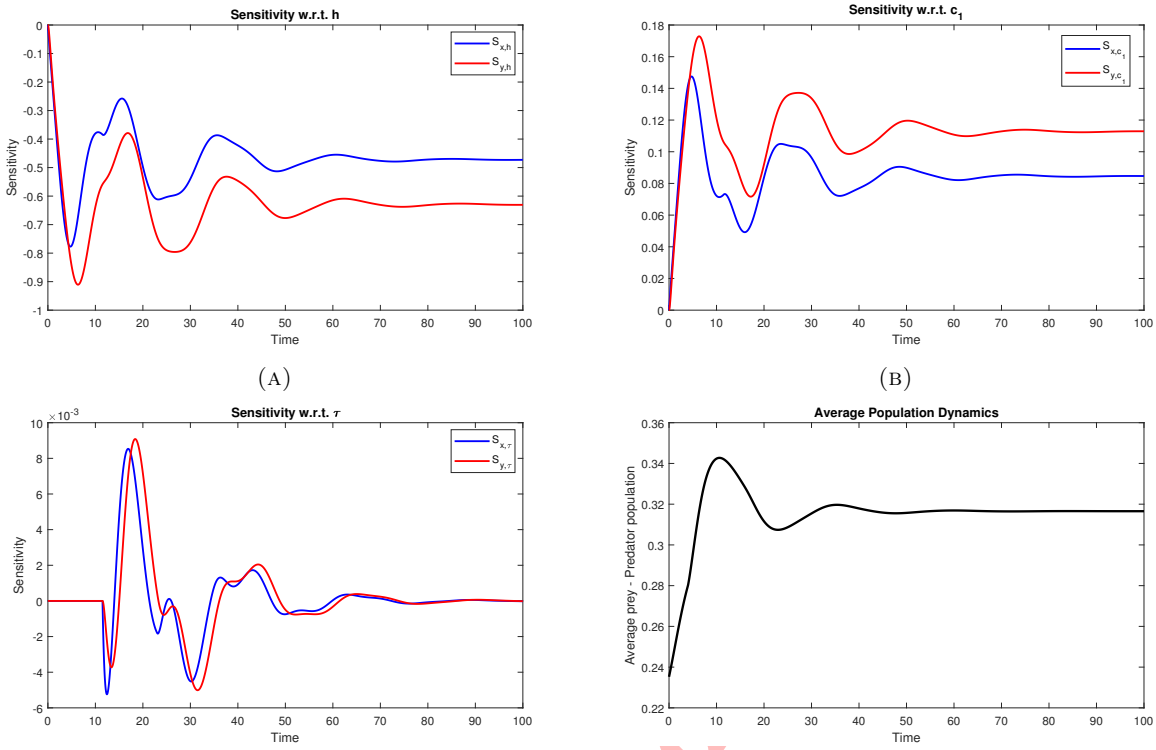

(A) (B)

(C) (D)

FIGURE 11. Sensitivity analysis with respect to the harvesting rate h, saturation parameter c_1, and delay τ on the population dynamics.

[22] F. A. Rihan and H. J. Alsakaji, *Stochastic delay differential equations of three-species prey-predator system with cooperation among prey species*, Discrete Contin. Dyn. Syst. Ser. S, *15*(2) (2022), 245–260.

[23] A. K. Sethy, and J. Datta, *Hunting cooperation in prey-predator models: spatiotemporal patterns and bifurcation analysis with Holling type IV response*, Journal of Mathematical Modeling, *14*(2) (2026), 431–451.

[24] A. K. Sethy and J. Datta, *Spatio-temporal patterns using Holling type-IV in a predator-based disease with immune prey*, International Journal of Dynamical Systems and Differential Equations, *14*(6) (2026), 469–487.

[25] R. Singh and B. Sahoo, *Sensitivity and uncertainty analysis of harvested ecological models*, Environ. Modell. Softw., *170* (2024), 105021.

[26] R. K. Upadhyay, P. Roy, and J. Datta, *Complex dynamics of ecological systems under nonlinear harvesting: Hopf bifurcation and Turing instability*, Nonlinear Dyn., *79* (2015), 2251–2270.

[27] R. K. Upadhyay, V. Rai, and S. N. Raw, *Hopf bifurcation and pattern formation in a delayed predator-prey model with nonlinear harvesting*, Nonlinear Dyn., *111* (2024), 845–867.

[28] X. Wang and Q. Liu, *Maximum sustainable yield in delayed prey-predator systems*, Math. Biosci., *364* (2023), 109020.

[29] J. Xia, Z. Liu, R. Yuan, and S. Ruan, *The effects of harvesting and the delay on predator-prey systems with Holling type II functional response*, SIAM J. Appl. Math., *70*(4) (2009), 1178–1200.

[30] Z. Zhang, R. K. Upadhyay, and J. Datta,*Bifurcation analysis of a modified Leslie-Gower model with Holling type-IV functional response and nonlinear prey harvesting*, Adv. Differ. Equ., *2018* (2018), 127.

[31] L. Zhang, Y. Wang, and X. Li, *Dynamics of a harvested predator-prey system with nonlinear functional response*, Chaos Solitons Fractals, *168* (2023), 113199.